

The Relaxation Pathways of CdSe Nanoparticles Monitored with Femtosecond Time-Resolution from the Visible to the IR: Assignment of the Transient Features by Carrier Quenching

Clemens Burda,^{*,†} Stephan Link, Mona Mohamed, and Mostafa El-Sayed*

Laser Dynamics Laboratory, School of Chemistry and Biochemistry, Georgia Institute of Technology, Atlanta, Georgia 30332-0400

Received: June 27, 2001; In Final Form: October 4, 2001

The relaxation dynamics of photoexcited CdSe nanoparticles (NPs) were studied with femtosecond pump–probe spectroscopy in the spectral range from 450 nm to 5 μm . Thus, the intraband relaxation of the electron and the hole were monitored with femtosecond time resolution. The transition from delocalized electronic to localized defect states and the slower relaxation through the trapping sites (trap hopping mechanism) were followed by time-resolved emission on time scales from picoseconds to milliseconds in the spectral range from the visible into the mid-infrared. The spectral dynamics in the visible, near-infrared (NIR), and infrared (IR) range give a mechanistic picture about the relaxation pathway of the excited charge carriers in CdSe NPs. In addition, by using electron and hole quenchers to the photoexcited nanoparticles, we could assign the observed dynamics to the electron or the hole. In the visible range, bleach features (negative signals in the differential transient absorption measurements) were observed at early delay times with time components of 2 ps, 30 ps, and a long-lived component of ~ 200 ps. Based on the quenching experiments, the bleach could be assigned to contributions from the electron *and* the hole. In the NIR and IR spectral range, the transient signal for short delay times (< 1 ns) were positive (transient absorption). A decay time of 1.2 ps was found for the transient absorption observed in the NIR. With the carrier removal technique, it could be shown that the NIR signal is mainly due to hole transitions. The IR signal with lifetimes of 2 ps, 30 ps, and a long component of ~ 200 ps compares directly to the decay times observed in the visible spectral range. It therefore is also composed of contributions from electron *and* hole. Photoluminescence is observed in the visible range at 570 nm (near band edge recombination), in the NIR at 1000 nm (deep-trap emission), and in the IR region at 4.8 μm (deeper-trap emission) with lifetimes of 43 ns, 250 ns, and 1 μs , respectively. The lifetimes of the emission increased for longer monitoring wavelengths, suggesting that for the investigated sample, the carriers relax from the band edge into shallow traps and from there continue stepwise relaxation into lower energy sites (trap hopping mechanism).

Introduction

The investigation of II–VI semiconductor nanoparticles (NPs) is largely focused on their optical properties. This is certainly due to the fact that the most striking features of quantum confinement are easily observed by their optical properties, which change as a function of the particle size.^{1–11} Since the electronic wave function experiences quantum confinement for small particle sizes on the nanometer-size scale, these nanoparticles are often discussed as quantum dots.^{8–18} The absorption band and the photoluminescence of II–VI semiconductors shift to longer wavelength with increasing particle size in the range from clusters of tens of atoms with < 1 nm diameter⁶ up to larger particles of several thousand atoms with tens of nanometers diameter.^{1,7,9} The size dependence of the optical properties is of wide interest for many potential applications and much progress has been achieved in the preparation^{19–24} and investigation of QDs.^{24–37} Nevertheless, the carrier dynamics of the excited states in semiconductor NPs are still being actively investigated.

For bulk II–VI semiconductors, due to the efficient coupling of the dynamics of the charge carriers with the polarity of the

lattice, the relaxation rates are very fast and the conduction band edge is rapidly populated.³⁸ The high density of electronic and phonon states leads to the high nonradiative relaxation rates observed for bulk materials. For quantum dots the situation changes dramatically. First, the electronic energy levels are discretized with an energy spacing, which exceeds by an order of magnitude the phonon energies.^{18,19} This leads theoretically to a limited relaxation rate, called the “phonon bottleneck”.³⁹ Second, the portion of the atoms, which are influenced by surface defects, is drastically increased. For the smallest clusters, essentially every atom can be regarded as being a surface atom.⁶ Surface imperfections lead to additional competing relaxation pathways by trapping into surface defect sites and can accelerate the depopulation of the band edge.^{34–53} Third, the increased coupling of electron and hole wave functions in quantum dots could further increase the relaxation rate. The overall effect of changing NP properties on the relaxation dynamics is therefore still difficult to predict and experiments are needed to collect facts, which help to describe the complex decay pathway in quantum dots.

Klimov et al.^{34,35} measured the relaxation times in the NIR range up to 2 μm and found that in this spectral range the dynamics is mainly due to the relaxing hole. On the other hand, the energy spacing of hole states is actually expected to be in the hundreds of meV and therefore rather in the THz regime

* Author to whom correspondence should be addressed

[†] Present address: Chemistry Department, Case Western Reserve University, Cleveland, OH 44106.

than in the NIR. Moreover, Guyot-Sionnest reported^{54–56} transitions due to electrons in the mid-IR range. These findings led us to use the method of selective electron and hole removal^{57,58} in combination with femtosecond time-resolved spectroscopy in order to yield further experimental evidence for the assignments of the NIR and IR transients.

In this paper we describe the femtosecond relaxation dynamics over a wide energy range from 400 nm up to 5 μm . Lifetime components up to milliseconds were recorded in photoluminescence experiments. These measurements were possible due to a new setup, which allows now in parallel the measurement of femtosecond transients over the whole spectral range from UV to IR.⁵⁹

Experimental Section

CdSe nanoparticles were synthesized according to the procedure developed by Murray et al.¹⁹ The chemicals were purchased from Alfa and all procedural steps were conducted under an argon atmosphere. The solutions remain stable for months. The nanoparticles were isolated by adding 100 mL of methanol to the cooled reaction solution followed by centrifugation. Repeated methanol washings followed by centrifugation removed excess TOPO and achieved a CdSe nanoparticle powder, which was very soluble in toluene. The size distribution resulting from the above procedure was very narrow with a standard deviation of 10% (300 particles counted) and thus the particles were used without further size selective precipitation. Preparation of the CdSe NP benzoquinone composites were carried out by adding an excess of 1,4-benzoquinone to the CdSe NP toluene solution and sonicating for 10 s. Similarly, the CdSe NP 4-aminothiophenole was prepared by adding the phenol compound into the CdSe colloidal solution and stirring the solution for several seconds. During these procedures the samples were always kept under argon.

Our femtosecond setup described earlier⁵³ was extended to probe parallel to the visible range also in the NIR range up to 2.5 μm and in the IR range up to 10 μm . An amplified Ti-Sapphire laser system (Clark MXR CPA 1000) was pumped by a Diode Pumped Solid State Laser (Coherent Verdi) with 3 W pump power. This system produced laser pulses of 100 fs duration (HWM) and an energy of 900 μJ at 800 nm. The repetition rate was 1 kHz. A small part (4%) of the fundamental was used to generate a white light continuum in a 2 mm sapphire plate. The remaining laser light was used to pump a second harmonic generator (SHG) to produce 400 nm excitation pulses. An optical parametric amplifier (OPA) was used to generate tunable probe wavelengths outside the continuum range. As probe pulse we used either the idler wave of the OPA in the range of 1700 nm to 2500 nm or the difference frequency for probing at longer wavelengths up to 10 μm . The probe light was then split into a reference and a signal beam. After passing the monochromator (Acton Research) both beams were detected by two IR-sensitive photodiodes (EG&G). The kinetic traces were obtained using a sample-and-hold unit and a lock-in-amplifier (Stanford Research Systems). The lowest measurable optical densities (OD) changes were 1 mOD. For spectral measurements a LN cooled CCD camera (Princeton Instruments) attached to a spectrograph (Acton Research) was used. The group velocity dispersion of the white light continuum was compensated.

Emission spectra were recorded on a PTI QuantaMaster QM1 and emission lifetimes with the PTI TimeMaster attachment, using a gated photomultiplier as detector and a PTI GL-3300 Nitrogen Laser as excitation source. The near-infrared emission

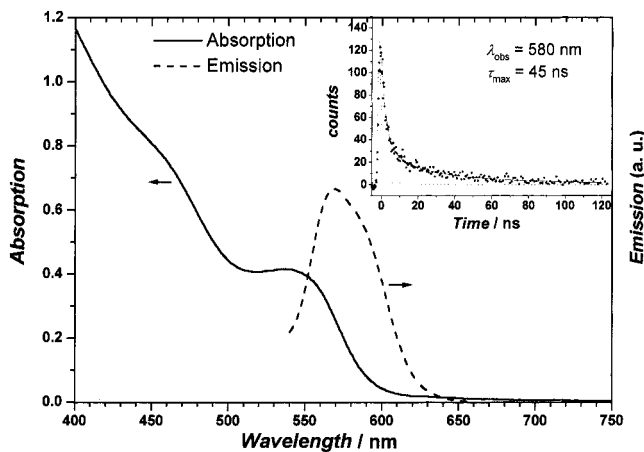


Figure 1. (a) The absorption spectrum of the CdSe NP sample is shown in solid line. The lowest allowed transition is observed at 560 nm. In dashed lines the corresponding emission, which peaks at 580 nm, is shown. The inset shows the decay trace of the emission observed at 580 nm. The decay curve could be fitted best with three exponentials with 3, 12, and 45 ns lifetime components. The dashed curve underneath represents the instrument's response function of 1.2 ns.

was detected with a Nicolet Magna 860 Raman spectrometer after excitation with a Coherent argon ion laser (Innova 300). The NIR emission lifetime was determined using a fast, liquid nitrogen cooled NIR photomultiplier from Hamamatsu (R5509-72). The mid-infrared emission was monitored with the Nicolet Magna 860 IR spectrometer. The IR emission lifetimes were recorded with the step-scan attachment unit by Nicolet.

Results

The colloidal CdSe nanoparticles (NPs) used in these experiments were characterized by UV absorption spectroscopy as shown in Figure 1. The absorption peak of the lowest allowed 1s1s exciton transition was located at 560 nm for these particles. At this wavelength, the bleach dynamics of the lowest allowed excitonic transition was investigated. Probe wavelengths of 2.0 μm and 4.8 μm were typically used to investigate intraband transitions of the NIR and IR regions. The photoluminescence of the CdSe sample shows a maximum at 580 nm. The shoulder at 585 nm indicates that in addition to band gap recombination a large portion of the excited carriers is trapped in various trapping sites. The dynamics of the band edge population and the following trapping processes are the objectives of the current study.

Femtosecond Transient Absorption. In our pump-probe experiment we measure the differential absorption at different delay times after excitation at 400 nm minus the ground state spectrum before excitation. This leads temporally to saturation of the ground-state transitions and therefore to a transient bleach at 560 nm. On the other hand, in the near-infrared (NIR) and in the infrared (IR) ranges, which are transparent in the ground state, the transient signals are positive. The femtosecond time-resolved pump-probe measurements were carried out in all three spectral ranges of the visible, the NIR, and the IR range. In Figure 2 three transient signals are presented which were measured in the different spectral regions after identical excitation conditions after excitation with 400 nm pulses of 0.8 μJ energy. It is shown that the bleaching at 560 nm and the transient absorption at 4800 nm are very similar in the dynamic response. Both traces were fitted with time constants of 2 and 30 ps. In contrast, the NIR signal decays much faster (1.2 ps) and is therefore assigned to a different process. Therefore we inves-

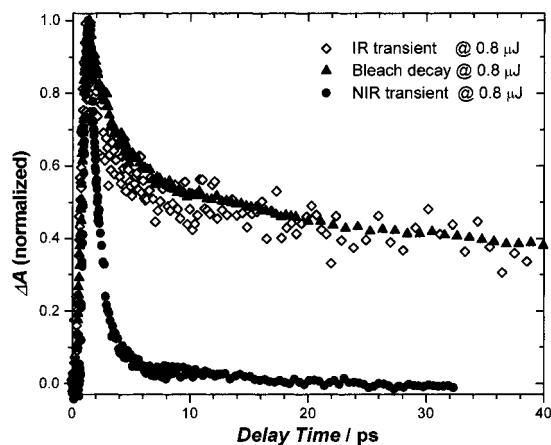


Figure 2. Femtosecond time-resolved kinetic traces which describe the response of the visible bleaching (570 nm probe wavelength, triangles), the IR (4.8 μm , open diamonds), and the NIR (1960 nm, solid circles) after excitation with 0.8 μJ at 400 nm. In this representation it becomes evident that the bleach (which actually is a negative signal) and the IR transient absorption occur on the same time scales (2 and 30 ps) and could be due to the same decay process. On the other hand, the NIR transient absorption seems to describe an independent event with a fast time constant of 1.2 ps.

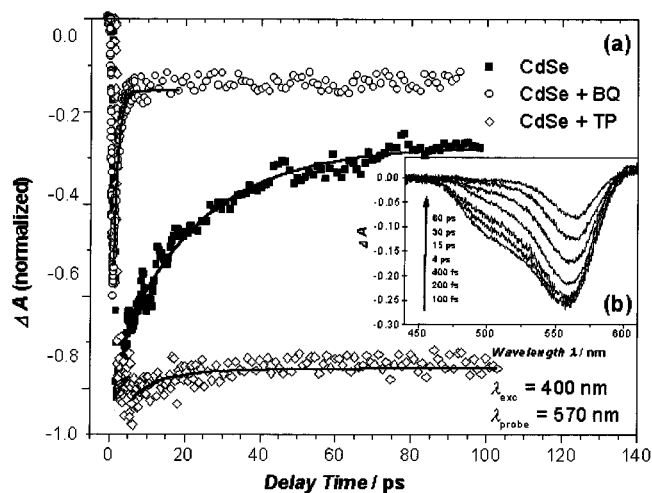


Figure 3. (a) The squares show the kinetic behavior of the bleach as monitored at 570 nm for CdSe nanoparticles without the addition of quenchers. The decay times are fitted to be 2 and 30 ps. After addition of benzoquinone (BQ) the bleach decay (circles) is accelerated to a monoexponential decay with a 2.7 ps lifetime. A weak off-set is observed for lower BQ concentrations, which is probably due to NPs which do not undergo electron transfer. Addition of 4-amino-thiophenol (TP) extends drastically the lifetime of the bleach (diamonds) due to hole trapping and elimination of electron traps. The time-resolved spectra in the visible spectral range are shown in the inset (b). The bleach maximum is reached after 200 fs at 560 nm.

igated the possibility that the dynamic response in the visible and in the IR describe the same processes, whereas the NIR dynamics could belong to an independent event. In addition, we collected evidence for an assignment of the observed dynamics to electron and hole relaxation processes, using the technique of electron and hole quenching.

UV–Vis Femtosecond Transient Bleach. The sample was excited with 400 nm femtosecond laser pulses. As illustrated in Figure 3a, the resulting bleach, which monitors the population of the lowest excitonic states, reaches its maximum at 560 nm 200 fs after excitation. The dynamics of the bleach was monitored at 570 nm, as illustrated in Figure 3a. The bleach

signal of CdSe NPs (squares) was found to decay with two components of 2 and 30 ps and a much longer component of ~ 200 ps.

By removing selectively and rapidly either the electron or the hole from the photoexcited nanoparticle (NP), it can be tested whether the bleach signal is determined by the electron or hole relaxation. As previously shown, this can be pursued by adding organic electron acceptors or electron donors to the NP solution, where the organic molecules are adsorbed on the NP surface.⁵³ We have chosen benzoquinone as electron acceptor (electron quencher, BQ) and 4-amino-thiophenol as electron donor (hole quencher, TP). The curve denoted as BQ (circles) shows the bleach dynamics after fast removal of the electron. It was shown before⁵³ that the addition of benzoquinone (BQ) to a colloidal solution of CdSe rapidly removes the electrons from the conduction band of the photoexcited NP and forms a short-lived charge transfer complex which monoexponentially decays with a lifetime of 2.7 ps. The repopulation of the ground state is thereby rate limited by the lifetime of the NP^+BQ^- charge transfer (CT) complex. Since the lifetime of the CT state is 2.7 ps, the excited-state lifetime of the CdSe–BQ conjugate is actually drastically shorter than the one of CdSe NP themselves. BQ removes the excited electron very efficiently, and acts like an additional electron trap. It is important to note, that after depopulating the conduction band edge and formation of the CT state, the spectral bleach at 560 nm is still observed in the time frame of 200 fs to 2.7 ps, until the CT state decays.⁵³ Therefore, the photoexcitation of an electron *and* its removal from the band edges cause a bleaching. When lower concentrations of BQ were used, incomplete quenching was observed. This could be due to incomplete conjugation of the NPs with BQ. Work on how the relaxation dynamics of the NP conjugates depends on the NP size and quencher concentration is currently in progress.

The addition of electron donor 4-amino-thiophenol (Figure 3a, diamonds) leads to a rapid neutralization of the photo-generated hole in the valence band.⁵⁵ The electron donor 4-amino-thiophenol (TP) can therefore be considered to be a hole quencher or hole trap. Furthermore, the addition of TP removes the electron traps on the NP surface. The excited state lifetime of CdSe NPs is considerably longer when TP was added and the bleach lifetime ($\gg 1$ ns) exceeds the time window of the femtosecond experiment. This finding was explained by the reduced electron–hole overlap⁵⁶ and by the fact that the TP would reduce the amount of electron surface traps.⁵⁵ The dynamic response, presented in Figure 3a, indicates that the electron, populating the conduction band edge, contributes to the transient bleach. But also the removal of an electron, which leaves back a p-doped NP, shows that the hole in the valence band also causes a part of the overall bleach in photoexcited samples. A quantitative estimation of each contribution is currently in progress.

Near-Infrared Femtosecond Transient Absorption. Excitation with 400 nm femtosecond pulses and monitoring in the NIR spectral range at 1960 nm results in a short-lived transient absorption with a 1.2 ps lifetime. Klimov et al.^{34,35} reported a 1.5 ps dynamics in this spectral range and assigned it to the relaxation of the hole. On the other hand, Guyot-Sionnest reported^{55,56} intraband electron transitions in the IR range from 2.5 to 5 μm . Therefore it was debated whether the features observed at even shorter wavelength (1900–2000 nm) could be due to the hole transitions. With the technique of selective removal of the excited electrons and holes we found additional experimental evidence that it is indeed the hole which gives

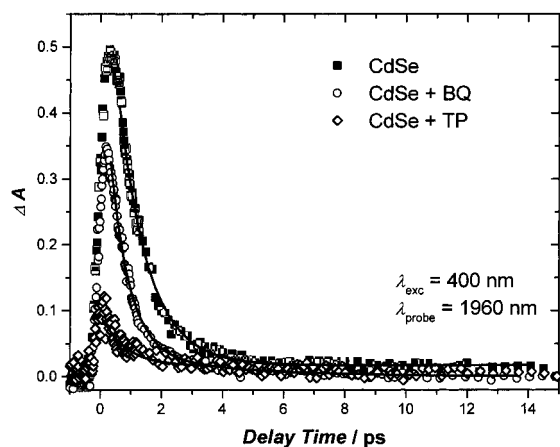


Figure 4. Relaxation dynamics of the transient absorption observed at 1960 nm in the NIR. The CdSe NP without quencher and the CdSeNP–BQ conjugate show the same relaxation dynamics with a 1.2 ps decay time. Therefore, it is likely that the transient is due to the relaxation of the hole. Indeed, the addition of hole quencher (TP) reduces the lifetime to 850 fs, which supports the assignment to a hole transition.

rise to the observed features at 1960 nm and that the previous findings do not contradict each other.

As seen in Figure 4, the transient observed for the CdSe NP solution without added quenchers (squares) at 1960 nm is indeed very short-lived and could be fitted monoexponentially with a 1.2 ps decay time. The addition of electron quencher BQ (circles) did not reduce the lifetime of the NIR transient absorption but the intensity of the transient was diminished to about 60% of the original transient intensity. In contrast, the addition of TP hole quencher (diamonds) reduces the lifetime of the transient absorption from 1.2 ps to 850 fs and the intensity is reduced by 80% of its original value. These results suggest that the NIR transient feature is mainly due to the hole, in accordance with the previous assignment by Klimov.^{34,35} Furthermore, based on the accelerated transient decay and $k_{\text{dec}} = \sum k_i$ (the sum of the individual relaxation processes), it can be estimated that the hole transfer to TP (trapping) is on the order of $k_{\text{ht}} \approx 3 \times 10^{11} \text{ s}^{-1}$. This requires a lifetime of the hole in the valence band of 3 ps or longer. Indeed, the quenching experiments with BQ already suggested that the hole lifetime is >2.7 ps. Furthermore, the hole trapping rate is reasonable, considered that the electron-transfer rate⁵³ to BQ is $k_{\text{et}} \geq 5 \times 10^{12} \text{ s}^{-1}$ and the hole has an effective mass which is several times larger than the effective electron mass for CdSe ($m_{\text{h}}/m_{\text{e}} \approx 6$).

Infrared Femtosecond Transient Absorption. On the basis of theory and NP size dependence of the transitions, the transient absorption in the IR wavelength range was previously assigned to the electronic intraband transition $1S_{\text{e}}-1P_{\text{e}}$.^{55,56} This transition was calculated by Guyot-Sionnest for different particle sizes including the Coulomb interactions within the particle.

Applying the electron and hole quenching to the observed IR transient adds further experimental evidence for this assignment. Upon 400 nm excitation of the CdSe NP sample without quenchers (squares) a transient absorption was observed when probing in the IR spectral range from 4000 to 5000 nm. The corresponding kinetic trace is shown in Figure 5. This CdSe NP solution shows a transient absorption signal that decays with 2 and 30 ps time constants. The electron quencher BQ (circles) reduces the long lifetime component of the transient from 30 to 12 ps. A clear quenching of the IR transient is observed and the short lifetime component of 2.6 ps appears, which we have

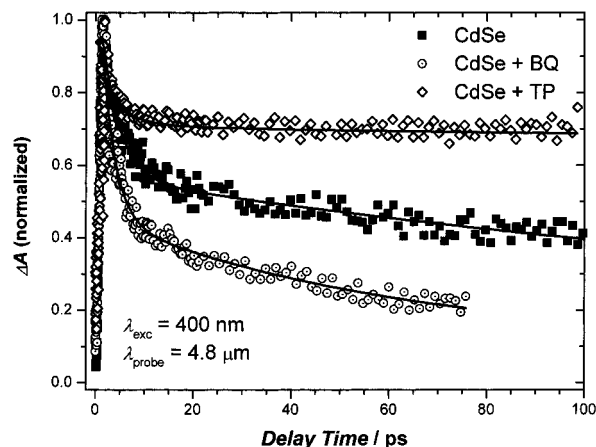


Figure 5. Relaxation dynamics of the transient absorption observed at 4.8 μm . The CdSe NP sample without quencher shows transients with 3 and 30 ps lifetimes. The CdSe–BQ sample relaxes faster with 2.6 and 12 ps lifetime components. In addition, the long lifetime contribution is partly quenched for the CdSe–BQ sample but clearly not quantitatively as was observed for the visible transient. The CdSe–TP conjugate shows long lifetimes of 2 ps and $\gg 100$ ps. Since the excited hole in the valence band is efficiently neutralized (trapped on the TP), the transient absorption in CdSe–TP is due to the remaining electron in the valence band. This dynamical behavior is very similar to the one observed for the bleach at 570 nm. Therefore, the transients are assigned to be mainly electron transitions.

previously assigned to the NP^+BQ^- CT complex. On the other hand, the transient absorption does not decay completely. This could be due to trap state absorption, which is possible on the longer time scales. In contrast to BQ, the addition of TP hole quencher (diamonds) leads to an extended lifetime. The effect of the additional quenchers on the monitored IR kinetics is very much like the one observed in the visible range (except that the observed transient at 4.8 μm is absorption and the transient at 570 nm is bleach). These quenching experiments confirm the assignment by Guyot-Sionnest that the IR transient absorption is, like the bleach, due to electronic transition in the conduction band.

Photoluminescence. The PL spectrum in Figure 1 is slightly broadened showing that the investigated sample predominantly relaxes via trap states. The photoluminescence (PL) lifetimes of CdSe NPs were monitored in all three spectral regions, visible (as shown in Figure 1 inset, dots), NIR (Figure 6), and IR (to be published elsewhere⁶⁰). Moreover, the technique of electron and hole quenching was applied to the PL processes and it is found that in all three spectral regions the addition of the BQ electron quencher as well as the addition of the TP quenches the emission quantitatively. Therefore, it needs both charge carriers in order to observe PL and it can be concluded that in all spectral regions under study the emission is due to radiative recombination of the carriers and not due to decoupled intraband transitions or phonon emission due to the relaxation of either one of the carriers. The PL decay monitored at 580 nm, with a time-resolution of 200 ps, showed three lifetime components of 2.8, 12.8, and 43 ns at RT. The PL quantum yield of the sample was 3% relative to Rhodamine 6 G in ethanol. From earlier measurements,⁵³ it is known that these PL lifetimes of our samples are limited due to surface trapping processes of the excited charge carriers. The longest lifetime observed at 580 nm reflects therefore the transition from the band edge or localized shallow trap states into lower-lying intraband gap states. The recombination of localized carriers occurs at lower energies and can therefore be observed in the NIR and IR range.

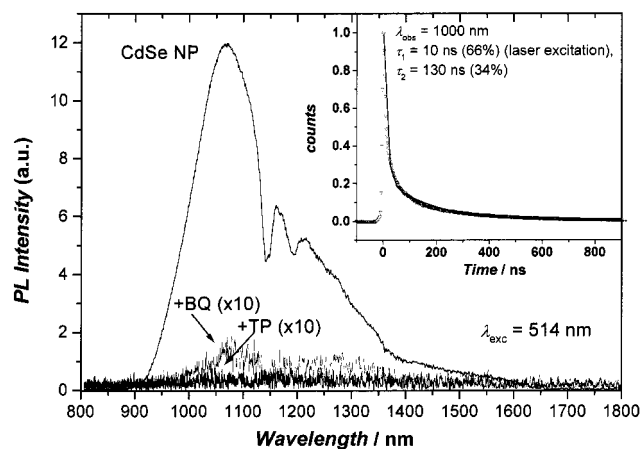


Figure 6. Photoluminescence (PL) spectra as observed in the NIR range. The PL could be quantitatively quenched when either BQ or TP was added. Therefore, the PL is due to carrier recombination. The NIR PL spectrum was recorded in a Raman spectrometer. The dips in the NIR PL spectrum are due to the solvent absorption lines of toluene. The spectral shape is influenced by the spectral sensitivity of the Raman system and is not corrected.

Steady-state PL measurements in the NIR range have been performed by exciting the CdSe NP sample with an Ar-ion laser line at 514.5 nm and monitoring the weak PL in a Raman spectrometer. The observed luminescence spectra are shown in Figure 6. The photoluminescence quantum yield in the NIR is estimated to be 0.3% relative to the laser dye Q-Switch 5 from Exciton in 1,2-dichloroethane. Since the bandwidth of the Raman system is spectrally limited, the shape of the PL bands is strongly influenced by the sensitivity of the detector. Nevertheless, it is evident that the CdSe NP sample shows significant radiative recombination in the spectral range of 900–1700 nm. The dips observed at 1140 and 1195 nm are due to vibrational lines of the solvent toluene. By using a liquid nitrogen cooled photomultiplier with a 3 ns response time, we measured a NIR PL lifetime of 130 ns at 1000 nm, as can be observed in the inset of Figure 6. The addition of BQ quenched the PL efficiently and also addition of TP led to PL quenching. The emission spectra in the IR range decay on the μ s time scale and are also efficiently quenched with either TP or BQ. The spectra and decay traces will be published elsewhere.⁶⁰

Discussion

The bleach in Figure 3b originates from the saturation of the lowest energy transitions. The rise and decay of the bleach is commonly discussed in terms of the band filling mechanism, which was proposed by Klimov et al.⁶¹ In the band filling picture, the excited charge carriers relax in a finite time through the many excited states and as a result the ground-state bleach experiences a red-shift, which corresponds to the relaxation rate to the band edges. For the electron this relaxation rate can be measured by the rise time of the bleach maximum, which is 200–400 fs. The hole relaxation can be correlated to the observed 1.2 ps decay of the NIR absorption. The observed 2 ps decay component (Figure 3a) could be due to additional Auger processes.⁶²

Figure 7 summarizes the electron-transfer dynamics when BQ or TP are added to the NP. Possible relaxation pathways are carrier recombination,⁴⁸ trapping,^{45–47} and population of the spin-forbidden dark state.^{63,64} The electron donor TP extends the initial bleach decay time to nanoseconds because the hole is efficiently trapped by TP and coupling to the hole is reduced. Moreover, the fast electron surface trapping processes are

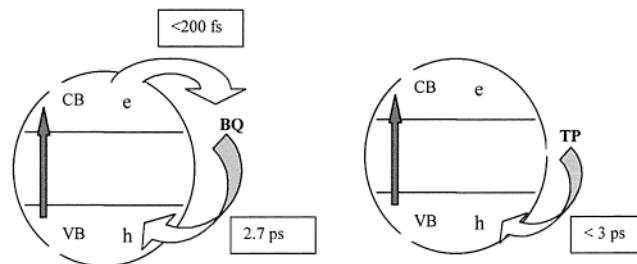


Figure 7. Scheme of the electron relaxation mechanism which takes place after benzoquinone (BQ) is attached to the CdSe NP surface (left side). BQ serves as an electron shuttle, which pumps the excited electron in < 3 ps from the conduction band back to the hole in valence band. The thiophenol (TP, right-hand side), is a hole trap (or electron donor) due to its low ionization potential. The hole transfer to TP is estimated to be on the order of 3 ps, on the basis of the quenching kinetics. This agrees with the fact that the lifetime of the hole on the conduction band edge is found to be longer than the NP+BQ⁻ lifetime (2.7 ps).

eliminated. On the other hand, the electron acceptor BQ accelerates the bleach decay since additional electron trapping is induced with the BQ on the NP surface. After removal of the conduction band electron, during the lifetime of the NP–BQ CT complex, (between 200 fs and 2.7 ps) the hole still occupies the valence band and the ground-state absorption is still bleached.⁵³ Therefore, the lifetime of the hole on the valence band edge has to be longer than the 2.7 ps lifetime of the NP–BQ CT complex. Also the removal of the hole by TP does not recover the bleach. Therefore, the quenching experiments with BQ and TP show that it is the electron occupying the conduction band *and* the hole populating the valence band that cause the excited CdSe NPs to be temporarily bleached and consequently it needs both carriers to be removed from the band edges for the ground-state absorption to be recovered.

The observed bleach lifetimes in the visible range have to be compared with the ones obtained from the transient absorption in the NIR and IR regions. Clearly, the NIR feature (Figure 4) decays with a monoexponential 1.2 ps lifetime much faster than the visible and IR features. The quenching experiments revealed that the 1.2 ps component at 1960 nm is due to an intraband transition of the hole. Since, the electron conduction band relaxation occurs within 400 fs, it seems that it is the hole relaxation which is rate limiting to the intraband relaxation process of the excited CdSe NPs.

In Figure 5, the dynamics in the IR region is shown for 4.8 μ m. Changes of the observation wavelength between 4 and 5 μ m did not lead to a change in the measured lifetimes of 2 and 30 ps. The fast decay components and the quenching results in the IR range compare well with the dynamics measured at 570 nm. The fastest components (2 ps) can be due to Auger processes, internal conversion, or trapping. On the other hand, the slowest components exceed the time window of our experimental setup. The long lifetime of the remaining transient absorption at 4.8 μ m could be due to trap-state absorption, similar to what Zhang et al. have reported in their visible-pump NIR-probe experiments for several different semiconductor NPs.^{50–52} On the other hand, Guyot-Sionnest²⁶ and Greenham⁶⁵ report long-lived electronic states, which were observed in the IR range. One difference can be found in the sample characteristics. It seems that the CdSe NP samples prepared in different groups show different surface properties and therefore result in different relaxation dynamics. The CdSe NPs prepared in our groups relax predominantly via trap states.

The transients observed in the femtosecond time-resolved pump–probe measurements occur on a much faster time scale

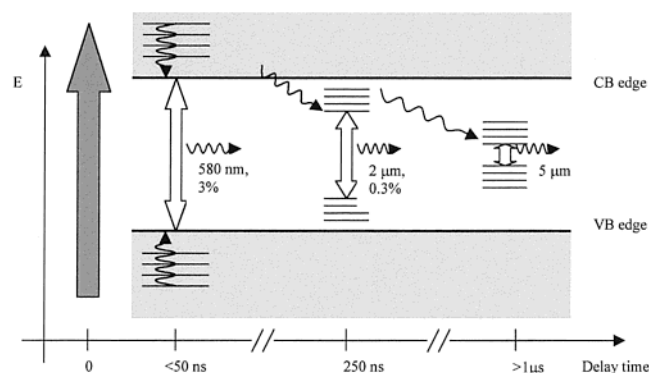


Figure 8. Scheme that summarizes the relaxation process observed by time-resolved transient absorption and photoluminescence spectroscopy in the spectral range from 450 to 5000 nm. The PL decay times are 43 ns, 130 ns, and $\sim 1\ \mu\text{s}$ at 580 nm, 1000 nm, and $5\ \mu\text{m}$ emission wavelength, respectively.

(picoseconds) than the PL lifetimes (nanoseconds). Therefore, the earlier seem to reflect components of the intraband relaxation of electrons and holes monitored by their intraband transitions, potentially influenced by some fast trapping or Auger processes. On the other hand, PL observed at the different observation wavelengths suggests a relaxation pathway from delocalized states to trap states with increasing emission wavelengths for longer delay times, as illustrated in Figure 8. At 580 nm the longest observed PL time constant is 43 ns. At 1000 nm the recombination occurs on a time scale of 130 ns and at $5\ \mu\text{m}$ the observed PL decays on a time-scale of $\sim 1\ \mu\text{s}$.⁶⁰ This suggests that recombination at lower energies occurs due to stepwise trap hopping into lower energy states on the NP surface. The time-resolution of our experiments was unfortunately not sufficient to resolve the rise times of the long-wavelength luminescence. A fast rise time in all spectral ranges would show that not only sequential trap hopping takes place but also fast and direct population of the deeper trapping sites. This question could be answered using a fluorescence up-conversion technique or utilizing a streak camera. It should be noted that Ekimov et al.⁶⁶ previously reported on the size-dependent luminescence of CdS nanoparticles in a glass matrix which extended from the visible to the NIR. They assigned the luminescence to band-impurity and inter-impurity transitions with lifetimes in the microsecond range. Furthermore, they found that with decreasing particle size the inter-impurity transitions dominate. Our suggested mechanism involving the luminescence originating from trap sites is in agreement with these studies since the electron and hole traps sites can be regarded as impurities.

In summary, we have measured the transient absorption and emission over the spectral range from 450 to 5000 nm. This measurement was made possible through an extensive addition on our femtosecond pump-probe system, which now allows measurements in the UV, NIR, and IR range in a short time. This was essential for this study since the limited lifetime of the prepared NP conjugates enforces a rapid change from detection in the visible to NIR or IR. The short lifetimes of the transients and their quencher dependence strongly suggest that the fast dynamics is due to band edge population and subsequent depopulation to surface traps. The conduction band edge population by the electron occurs within 200–400 fs (bleach rise time) when CdSe NPs are excited at 400 nm. Under the same excitation conditions, the hole relaxes within 1.2 ps (NIR absorption decay) to the valence band edge and remains there for $> 3\ \text{ps}$ (NP-BQ CT lifetime). At longer times, induced absorptions are due to trap state transitions, as was observed in

the NIR range by Zhang et al.^{50–52} The PL occurring on the nanosecond time scale is therefore assigned to radiative recombination from trap states. The PL red-shifts drastically for longer observation times which is strong experimental evidence for a trap hopping mechanism into subsequently lower trap states.

Acknowledgment. The continued support of this work by the Office of Naval Research (ONR Grant No. CHE-9727633) is greatly appreciated. S.L. gratefully acknowledges the partial support by the MDI (ONR Grant No. N00014-95-1-0306) at Georgia Tech. The authors thank Dr. J. P. Wang and Prof. P. Guyot-Sionnest for valuable discussions.

References and Notes

- (1) Brus, L. E. *J. Lumin.* **1984**, *31&32*, 381.
- (2) Weller, H.; Koch, U.; Gutierrez, M.; Henglein, A. *Ber. Bunsen-Ges. Phys. Chem.* **1984**, *88*, 649.
- (3) Weller, H.; Schmidt, H. M.; Koch, U.; Fojtik, A.; Baral, S.; Henglein, A.; Kunath, W.; Weiss, K.; Dieman, E. *Chem. Phys. Lett.* **1986**, *124*, 557.
- (4) Eychmueller, A.; Haesselbarth, A.; Katsikas, L.; Weller, H. *J. Lumin.* **1991**, *48&49*, 745.
- (5) Bawendi, M. G.; Wilson, W. L.; Rothberg, L.; Carroll, P. J.; Jedju, T. M.; Steigerwald, M. L.; Brus, L. E. *Phys. Rev. Lett.* **1990**, *65*, 1623.
- (6) Soloviev, V. N.; Eichhoefer, A.; Fenske, D.; Banin, U. *J. Am. Chem. Soc.* **2000**, *122*, 2673.
- (7) Mittleman, D. M.; Schoenlein, R. W.; Shiang, J. J.; Colvin, V. L.; Alivisatos, A. P.; Shank, C. V. *Phys. Rev. B* **1994**, *49*, 14435.
- (8) Norris, D. J.; Nirmal, M.; Murray, C. B.; Sacra, A.; Bawendi, M. G. *Z. Phys. D* **1993**, *26*, 355.
- (9) Norris, D. J.; Sacra, A.; Murray, C. B.; Bawendi, M. G. *Phys. Rev. Lett.* **1994**, *72*, 2612.
- (10) Jacobssohn, M.; Banin, U. *J. Phys. Chem. B* **2000**, *104*, 1.
- (11) Ekimov, A. I.; Onushchenko, A. A. *J. JETP Lett.* **1981**, *34*, 345.
- (12) Woggon, U.; Gaponenko, S.; Langbein, W.; Uhrig, A.; Klingshirn, C. *Phys. Rev. B* **1993**, *47*, 3684.
- (13) Woggon, U.; Saleh, M.; Uhrig, A.; Portune, M.; Klingshirn, C. *J. Cryst. Growth* **1994**, *138*, 988.
- (14) Gaponenko, S. V.; Woggon, U.; Uhrig, A.; Langbein, W.; Klingshirn, C. *J. Lumin.* **1994**, *60&61*, 302.
- (15) Wind, O.; Kalt, H.; Woggon, U.; Klingshirn, C. *Adv. Mater. Opt. Electron.* **1994**, *3*, 89.
- (16) Woggon, U.; Portune, M. *Phys. Rev. B* **1995**, *51*, 4719.
- (17) Woggon, U.; Portune, M.; Klingshirn, C.; Giessen, H.; Fluegel, B.; Mohs, G.; Peyghambarian, N. *Phys. Status Solidi B* **1995**, *188*, 221.
- (18) Woggon, U.; Wind, O.; Gindele, F.; Tsitsishvili, E.; Mueller, M. *J. Lumin.* **1996**, *70*, 269.
- (19) Murray, C. B.; Norris, D. J.; Bawendi, M. G. *J. Am. Chem. Soc.* **1993**, *115*, 8706.
- (20) Peng, Z. A.; Peng, X. *J. Am. Chem. Soc.* **2001**, *123*, 183.
- (21) Gao, M.; Kirstein, S.; Moehwald, H.; Rogach, A. L.; Kornowski, A.; Eychmueller, A.; Weller, H. *J. Phys. Chem. B* **1998**, *102*, 8360.
- (22) Rogach, A.; Kershaw, S.; Burt, M.; Harrison, M.; Kornowski, A.; Eychmueller, A.; Weller, H. *Adv. Mater.* **1999**, *11*, 552.
- (23) Hines, M. A.; Guyot-Sionnest, P. *J. Phys. Chem. B* **1998**, *102*, 3655.
- (24) Braun, M.; Burda, C.; El-Sayed, M. A. *J. Phys. Chem. B* **2001**, *105*, 5548.
- (25) Klimov, V. I. *J. Phys. Chem. B* **2000**, *104*, 6112.
- (26) Shim, M.; Shilov, S. V.; Braiman, M. S.; Guyot-Sionnest, P. *J. Phys. Chem. B* **2000**, *104*, 1494.
- (27) Underwood, D. F.; Kippenny, T.; Rosenthal, S. J. *J. Phys. Chem. B* **2001**, *105*, 436.
- (28) Lami, J.-F.; Hirlimann, C. *Phys. Rev. B* **1999**, *60*, 4763.
- (29) Alivisatos, A. P.; Harris, A. L.; Levinos, N. J.; Steigerwald, M. L.; Brus, L. E. *J. Chem. Phys.* **1988**, *89*, 4001.
- (30) Burda, C.; El-Sayed, M. A. *Pure Appl. Chem.* **2000**, *72*, 165.
- (31) Burda, C.; Green, T.; Landes, C.; Link, S.; Little, R.; Petroski, J.; El-Sayed, M. A. In *Characterization of Nanophase Materials*; Wang, Z. L., Ed.; Wiley-VCH: New York, 2000.
- (32) Tittel, J.; Goehde, W.; Koberling, F.; Basche, Th.; Kornowski, A.; Weller, H.; Eychmueller, A. *J. Phys. Chem. B* **1997**, *101*, 3013.
- (33) Empedocles, S.; Bawendi, M. *Acc. Chem. Res.* **1999**, *32*, 389.
- (34) Klimov, V. I.; Schwarz, Ch. J.; McBranch, D. W.; Leatherdale, C. A.; Bawendi, M. G. *Phys. Rev. B* **1999**, *60*, R2177.
- (35) Klimov, V. I.; McBranch, D. W.; Leatherdale, C. A.; Bawendi, M. G. *Phys. Rev. B* **1999**, *60*, 13740.
- (36) Klimov, V. I.; McBranch, D. W. *Phys. Rev. Lett.* **1998**, *80*, 4028.

- (37) Klimov, V. I.; Mikhailovsky, A. A.; McBranch, D. W.; Leatherdale, C. A.; Bawendi, M. G. *Phys. Rev. B* **2000**, *61*, R13349.
- (38) Shah, J. *Ultrafast spectroscopy of semiconductors and semiconductor nanostructures*; Springer: New York, 1999.
- (39) Helm, U.; Wiesner, P. *Phys. Rev. Lett.* **1973**, *30*, 1205.
- (40) Rossetti, R.; Brus, L. E. *J. Phys. Chem.* **1982**, *86*, 4470.
- (41) Chestnoy, N.; Harris, T. D.; Hull, R.; Brus, L. E. *J. Phys. Chem.* **1986**, *90*, 3393.
- (42) Kaschke, M.; Ernsting, N. P.; Mueller, U.; Weller, H. *Chem. Phys. Lett.* **1990**, *168*, 543.
- (43) Henglein, A.; Gutierrez, M.; Fischer, C. H. *Ber. Bunsen-Ges. Phys. Chem.* **1984**, *88*, 170.
- (44) Spanhel, L.; Haase, M.; Weller, H.; Henglein, A. *J. Am. Chem. Soc.* **1987**, *109*, 5649.
- (45) Bawendi, M. G.; Carroll, P. J.; Wilson, William, L.; Brus, L. E. *J. Chem. Phys.* **1992**, *96*, 946.
- (46) Nirmal, M.; Murray, C. B.; Norris, D. J.; Bawendi, M. G. *Z. Phys. D* **1993**, *26*, 361.
- (47) Nirmal, M.; Murray, C. B.; Bawendi, M. G. *Phys. Rev. B* **1994**, *50*, 2293.
- (48) Kuno, M.; Lee, J. K.; Dabbousi, B. O.; Mikulec, F. V.; Bawendi, M. G. *J. Chem. Phys.* **1997**, *106*, 9869.
- (49) Haesselbarth, A.; Eychmueller, A.; Weller, H. *Chem. Phys. Lett.* **1993**, *203*, 271.
- (50) Zhang, J. Z.; O'Neil, R. H.; Roberti, T. W.; McGowen, J. L.; Evans, J. E. *Chem. Phys. Lett.* **1994**, *218*, 479.
- (51) Zhang, J. Z.; O'Neill, R. H.; Roberti, T. W. *Appl. Phys. Lett.* **1994**, *64*, 1989.
- (52) Zhang, J. Z. *J. Phys. Chem. B* **2000**, *104*, 7239.
- (53) Burda, C.; Green, T. C.; Link, S.; El-Sayed, M. A. *J. Phys. Chem. B* **1999**, *103*, 1783.
- (54) Guyot-Sionnest, P. Private communications.
- (55) Guyot-Sionnest, P.; Shim, M.; Matranga, C.; Hines, M. *Phys. Rev. B* **1999**, *60*, R2181.
- (56) Guyot-Sionnest, P.; Hines, M. A. *Appl. Phys. Lett.* **1998**, *72*, 686.
- (57) Burda, C.; Link, S.; Green, T. C.; El-Sayed, M. A. *J. Phys. Chem. B* **1999**, *103*, 10775.
- (58) Burda, C.; Green, T. C.; Link, S.; El-Sayed, M. A. *Proceedings of the Materials Research Society, Microcrystalline and Nanocrystalline Semiconductors* **1999**, 536, 419.
- (59) Link, S.; Burda, C.; Braun, M.; Logunov, S.; El-Sayed, M. A. To be published.
- (60) Mohammed, M.; Wang, J. P.; El-Sayed, M. A. To be published.
- (61) Klimov, V. I. In *Handbook on Nanostructured Materials and Nanotechnology*; Nalwa, H., Ed.; Academic Press: San Diego, CA, 1999; Vol. 4, p 451.
- (62) Klimov, V. I.; Mikhailovsky, A. A.; McBranch, D. W.; Leatherdale, C. A.; Bawendi, M. G. *Science* **2000**, *287*, 1011.
- (63) Efros, Al. L.; Rosen, M.; Kuno, M.; Nirmal, M.; Norris, D. J.; Bawendi, M. *Phys. Rev. B* **1996**, *54*, 4843.
- (64) Nirmal, M.; Norris, D. J.; Kuno, M.; Bawendi, M. G.; Efros, Al. L.; Rosen, M. *Phys. Rev. Lett.* **1995**, *75*, 3728.
- (65) Ginger, D. S.; Dhoot, A. S.; Finlayson, C. E.; Greenham, N. C. *Appl. Phys. Lett.* **2000**, *77*, 2816.
- (66) Ekimov, A. I.; Kudryavtsev, I. A.; Ivanov, M. G.; Efros, Al. L. *J. Lumin.* **1990**, *46*, 83.